

Supplementary information for:  
**Resetting proteostasis with ISRIB promotes epithelial differentiation  
to attenuate pulmonary fibrosis**

Satoshi Watanabe, Nikolay S. Markov, Ziyang Lu, Raul Piseaux Aillon, Saul Soberanes, Constance E. Runyan, Ziyou Ren, Rogan A. Grant, Mariana Maciel, Hiam Abdala-Valencia, Yuliya Politanska, Kiwon Nam, Lango Sichizya, Hermon G. Kihshen, Nikita Joshi, Alexandra C. McQuattie-Pimentel, Katherine A. Gruner, Manu Jain, Jacob I. Sznajder, Richard I. Morimoto, Paul A. Reyfman, Cara J. Gottardi, G.R. Scott Budinger, Alexander V. Misharin

Corresponding authors:

G.R. Scott Budinger

E-mail: s-buding@northwestern.edu

Alexander V. Misharin

E-mail: a-misharin@northwestern.edu

**This PDF file includes:**

Figures S1-S7

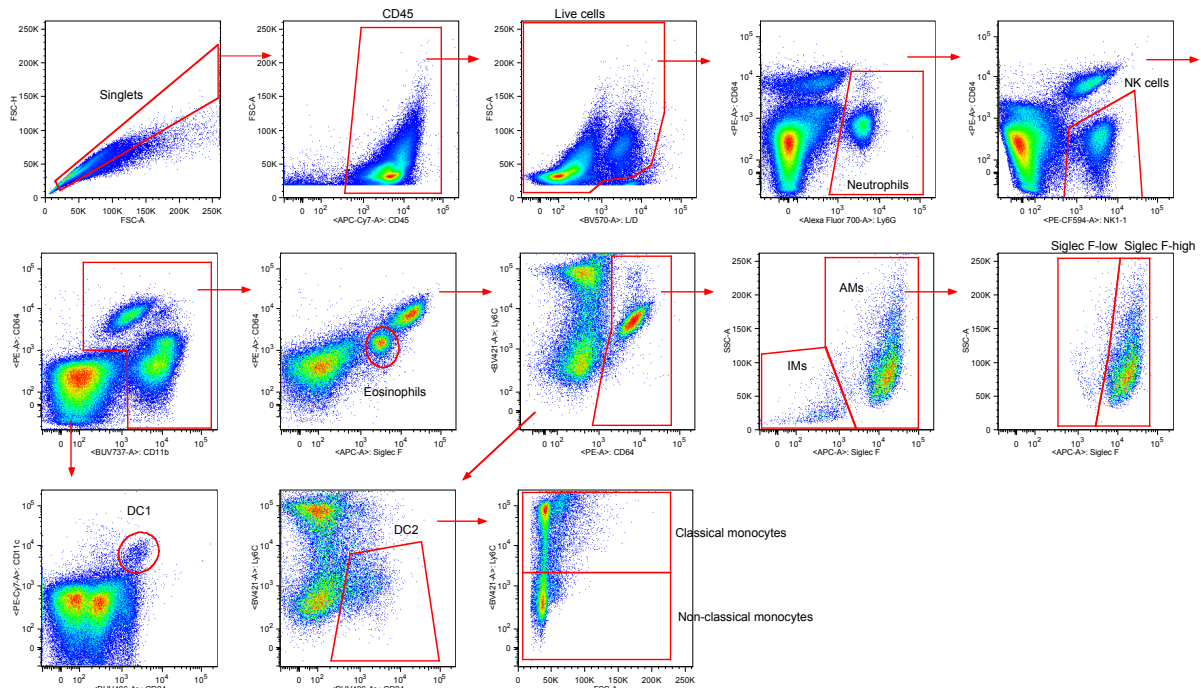
Table S1

**Other supplementary materials for this manuscript include the following:**

Datasets S1–S5

## SUPPLEMENTAL FIGURES AND TABLES

### A Gating strategy (myeloid cells)



### B Gating strategy (lymphoid cells)

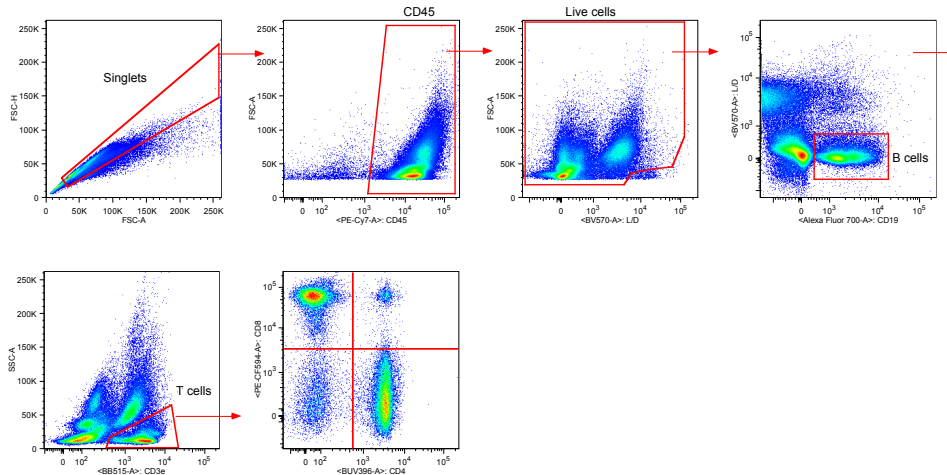


**Figure S1. Gating strategy used to identify myeloid and lymphoid cell populations in single cell suspensions from the whole lung.** Gating strategy for myeloid cell populations (A) and lymphoid cell populations (B). Representative flow cytometry plots from a naïve young adult mouse lung are shown.

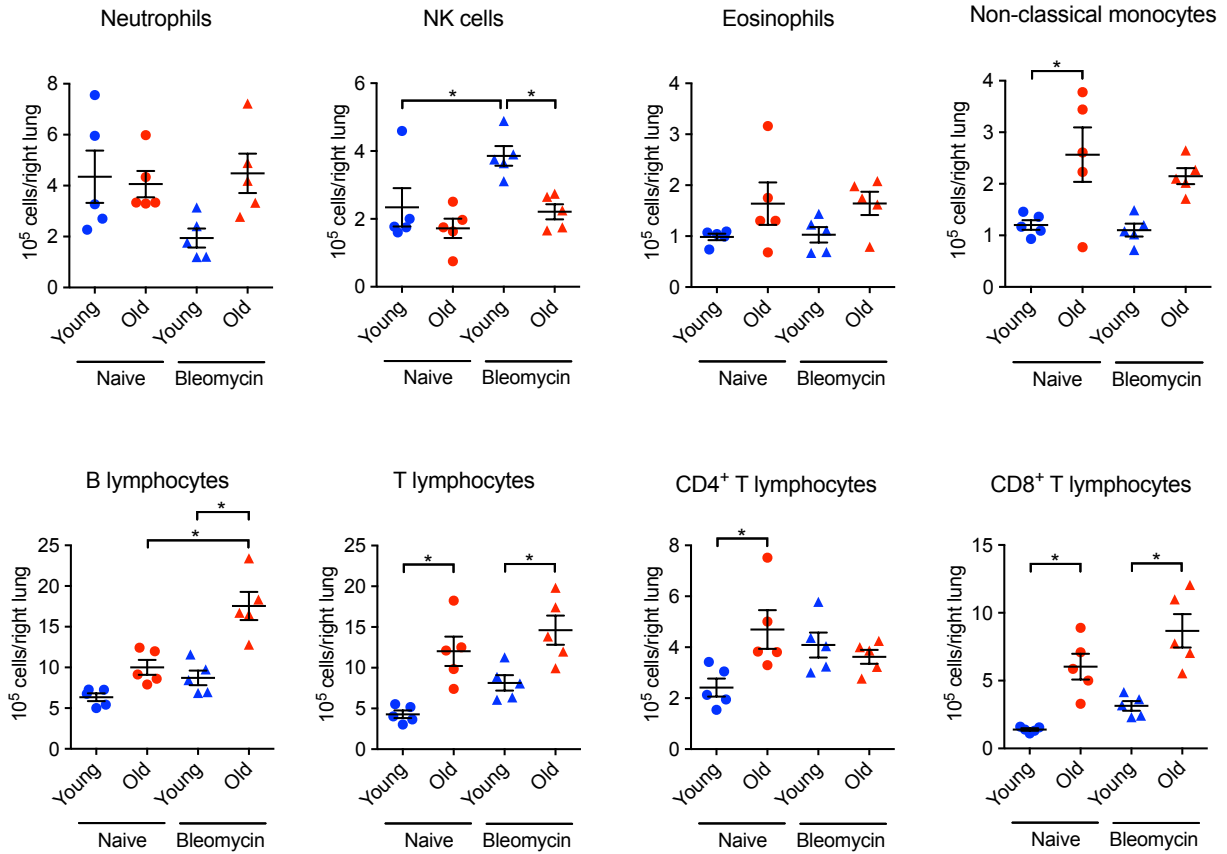


**Figure S2. Lung lymphoid and myeloid cell populations in young adult and old mice.** Young adult mice (3–5 months) and old mice (18–24 months) were administered bleomycin (0.025 unit/50  $\mu$ l, intratracheally) and the lungs were harvested 28 days later. Myeloid populations including neutrophils, eosinophils and non-classical monocytes and lymphoid populations including B cells, CD4<sup>+</sup> T cells, CD8<sup>+</sup> T cells, and NK cells, were enumerated using flow cytometry. Data presented as mean  $\pm$  SEM, 5–8 mice per group, one-way ANOVA with Tukey test for multiple comparisons. \*,  $p < 0.05$ .

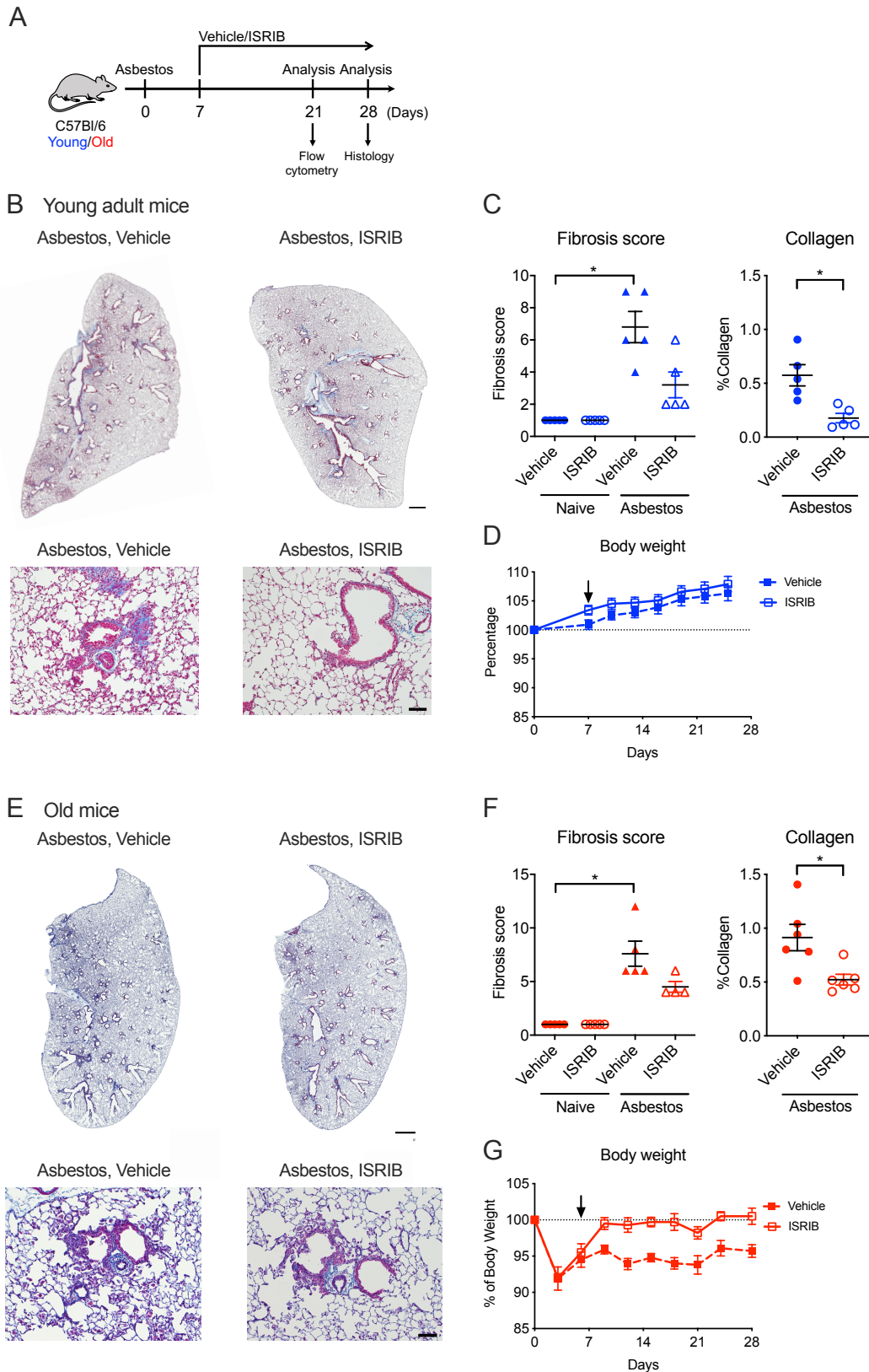


**Figure S3. Therapy with ISRIB attenuates asbestos-induced lung fibrosis in young adult and old mice.** (A) Schematic of the experimental design. Young adult (3–5 months) and old (18–24 months) mice

were administered crocidolite asbestos (100  $\mu\text{g}/50 \mu\text{l}$ , intratracheally) and treated with 2.5 mg/kg of ISRIB or vehicle (i.p., every day) beginning at day 7 and harvested at the indicated time points. **(B, E)** Representative images of lung tissue from naïve or asbestos-treated young adult **(B)** or old **(E)** mice with or without ISRIB on day 28. Masson's trichrome staining. Scale bar = 1 mm. Representative images in high magnification are also shown. Scale bar = 100  $\mu\text{m}$ . **(C, F)** Ashcroft fibrosis score (Mann-Whitney tests with Bonferroni multiple test correction) and relative collagen levels using second harmonic generation (Mann-Whitney test) from naïve mice or asbestos-treated mice with or without ISRIB. **(D, G)** Body weight. Arrow indicates start of ISRIB treatment (one-way ANOVA with Dunnett's multiple comparisons test). Data are shown as mean  $\pm$  SEM, 5–7 mice per group. \*  $p < 0.05$ . Representative data from one of two independent experiments are shown.

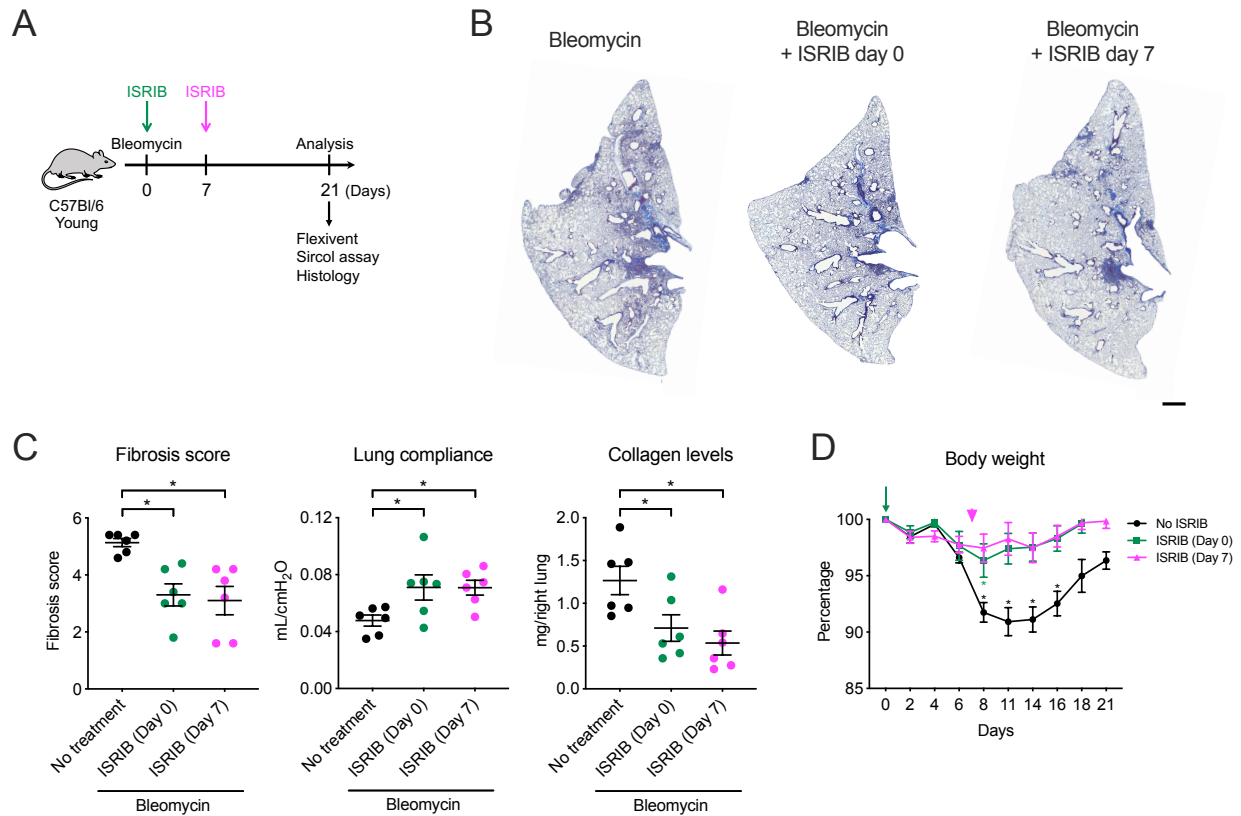


**Figure S4. A single dose of ISRIB ameliorates lung fibrosis.** (A) Schematic of the experimental design. Young adult (3–5 months) mice were administered 0.025 unit of bleomycin and treated with a single dose of ISRIB (2.5 mg/kg) simultaneously or 7 days later. (B) Representative Masson's trichrome stained lung sections (scale bar = 1 mm). (C) Ashcroft fibrosis score, lung compliance (Flexivent), and soluble collagen in lung homogenates. One-way ANOVA with Dunnett's test for multiple comparisons. (D) Body weight. Arrows indicate ISRIB treatment. one-way ANOVA with Dunnett's multiple comparisons test, comparing data from each day to baseline (day 0). Data are shown as mean  $\pm$  SEM, 6 mice per group. \*  $p < 0.05$ .

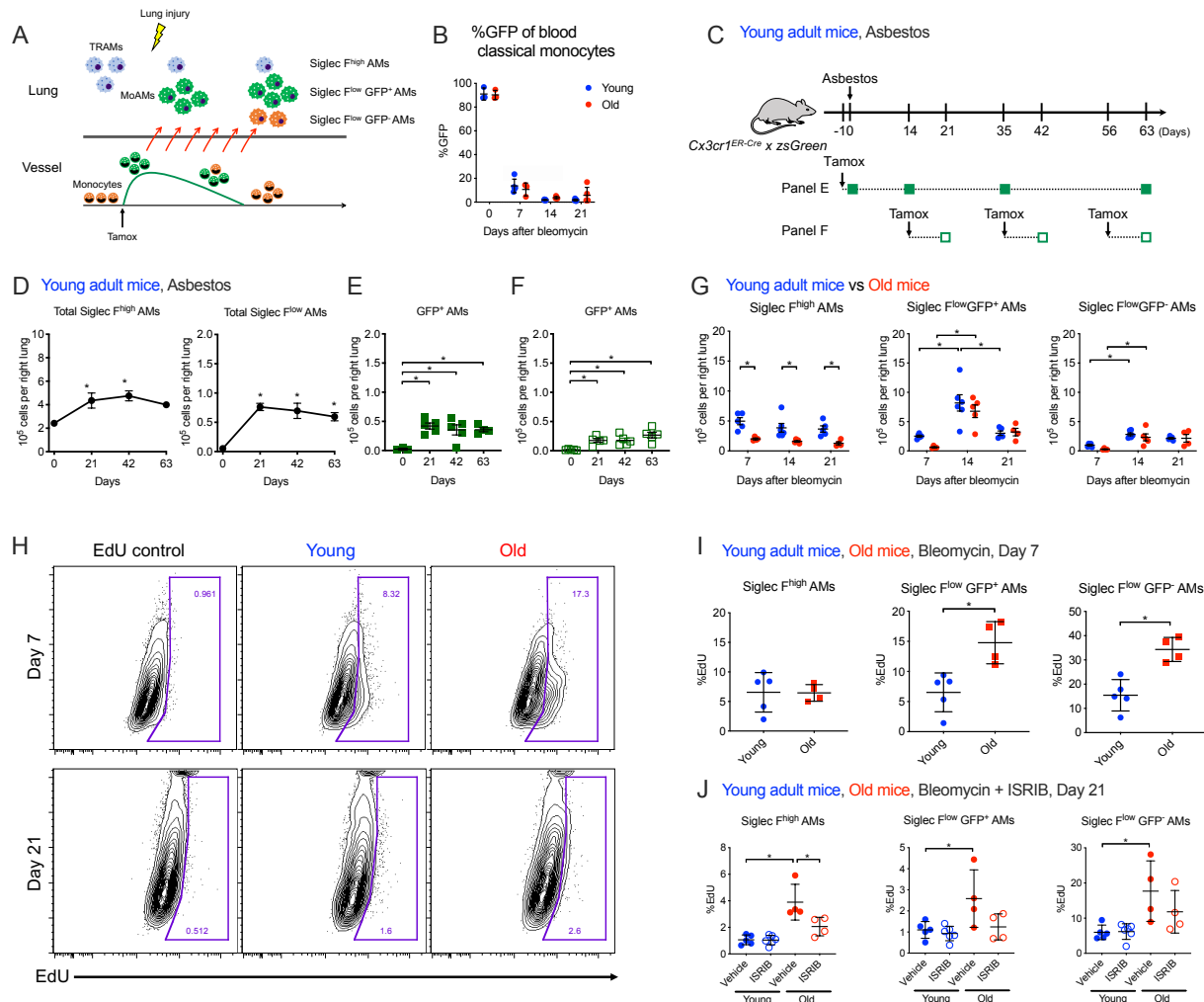
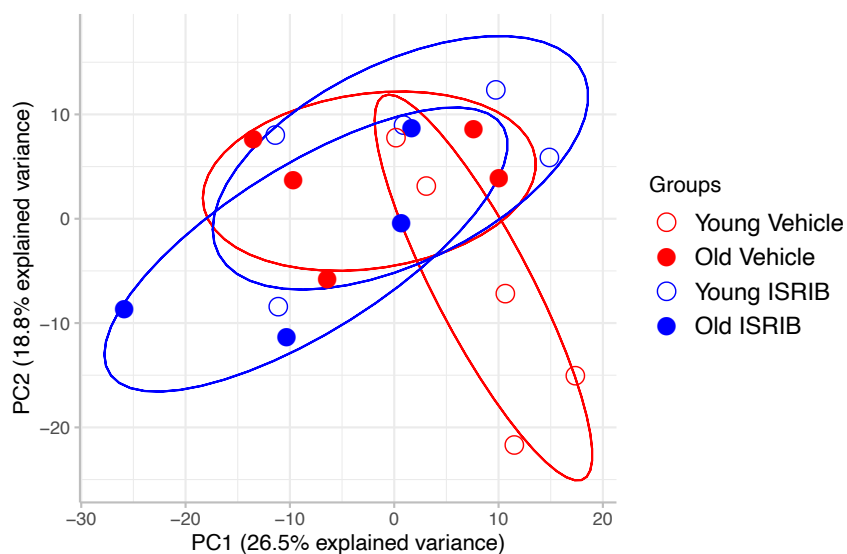


**Figure S5. The recruitment kinetics of monocyte-derived alveolar macrophages in young adult and old mice during lung fibrosis.** (A) Schematic of the *Cx3cr1*<sup>ERCre</sup> × *zsGreen* lineage tracing system to assess recruitment of monocyte-derived alveolar macrophages. (B) Percentage of GFP-positive circulating monocytes during the course of bleomycin-induced lung fibrosis after a single dose of tamoxifen administered one day prior to bleomycin in young adult and old *Cx3cr1*<sup>ERCre</sup> × *zsGreen* mice. (C) Schematic of the genetic lineage tracing system in the asbestos lung fibrosis model. (D) The number of total Siglec F<sup>high</sup> alveolar macrophages (AMs), Siglec F<sup>low</sup> AMs in the asbestos model. One-way ANOVA with Dunnett's test for multiple comparisons. (E) Monocyte-derived alveolar macrophages recruited during the first week after asbestos instillation persist during the course of asbestos-induced fibrosis (one-way ANOVA with Dunnett's test for multiple comparisons, compared to day 0). *Cx3cr1*<sup>ERCre</sup> × *zsGreen* mice received a pulse of tamoxifen one day prior to instillation of asbestos and were analyzed at indicated time points. No significant difference between the number of GFP+ monocyte-derived alveolar macrophages between days 21, 42 and 63. (F) Recruitment of monocyte-derived alveolar macrophages continues through the course of asbestos-induced fibrosis. *Cx3cr1*<sup>ERCre</sup> × *zsGreen* mice were intratracheally instilled with asbestos and were treated with a pulse of tamoxifen 7 days prior to analysis at indicated time points. No significant difference between the number of GFP+ monocyte-derived alveolar macrophages between days 21, 42 and 63, one-way ANOVA with Dunnett's test for multiple comparisons. (G) Young (3–5 months) and old (18–24 months) *Cx3cr1*<sup>ERCre</sup> × *zsGreen* mice have similar kinetics of monocyte-derived alveolar macrophage recruitment in bleomycin-induced lung fibrosis. Tamoxifen was administered one day to

intratracheal instillation of bleomycin and mice were treated and harvested at the indicated time-points. Two-way ANOVA with Tukey's test for multiple comparisons. **(H)** Representative contour plots showing EdU incorporation in Siglec F<sup>low</sup>GFP<sup>+</sup> alveolar macrophages. **(I)** EdU incorporation into monocyte-derived alveolar macrophages in old mice. Mann-Whitney test. \*p < 0.05. **(J)** EdU incorporation into monocyte-derived alveolar macrophages with and without ISRIB treatment. Kruskal-Wallis test with Dunn's correction for multiple comparisons. \*p < 0.05. Data are shown as mean ± SEM.



### A Classical monocytes in naive mice



### B Siglec F<sup>low</sup> alveolar macrophages in bleomycin model

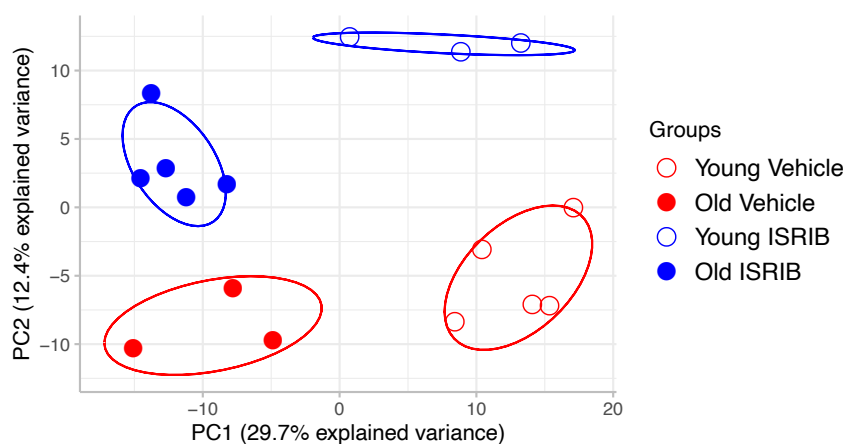


**Figure S6. Transcriptomic profiling does not reveal evidence of activation of the ISR in monocyte or alveolar macrophage populations in the lung. (A)** Principal component analysis of classical monocytes in young and old naïve mice treated with ISRIB or vehicle for 7 days did not reveal age- or treatment-related sources of variation. **(B)** Principal component analysis of CD64<sup>+</sup>Siglec F<sup>low</sup> monocyte-derived alveolar macrophages in young adult and old mice exposed to bleomycin with and without ISRIB treatment.

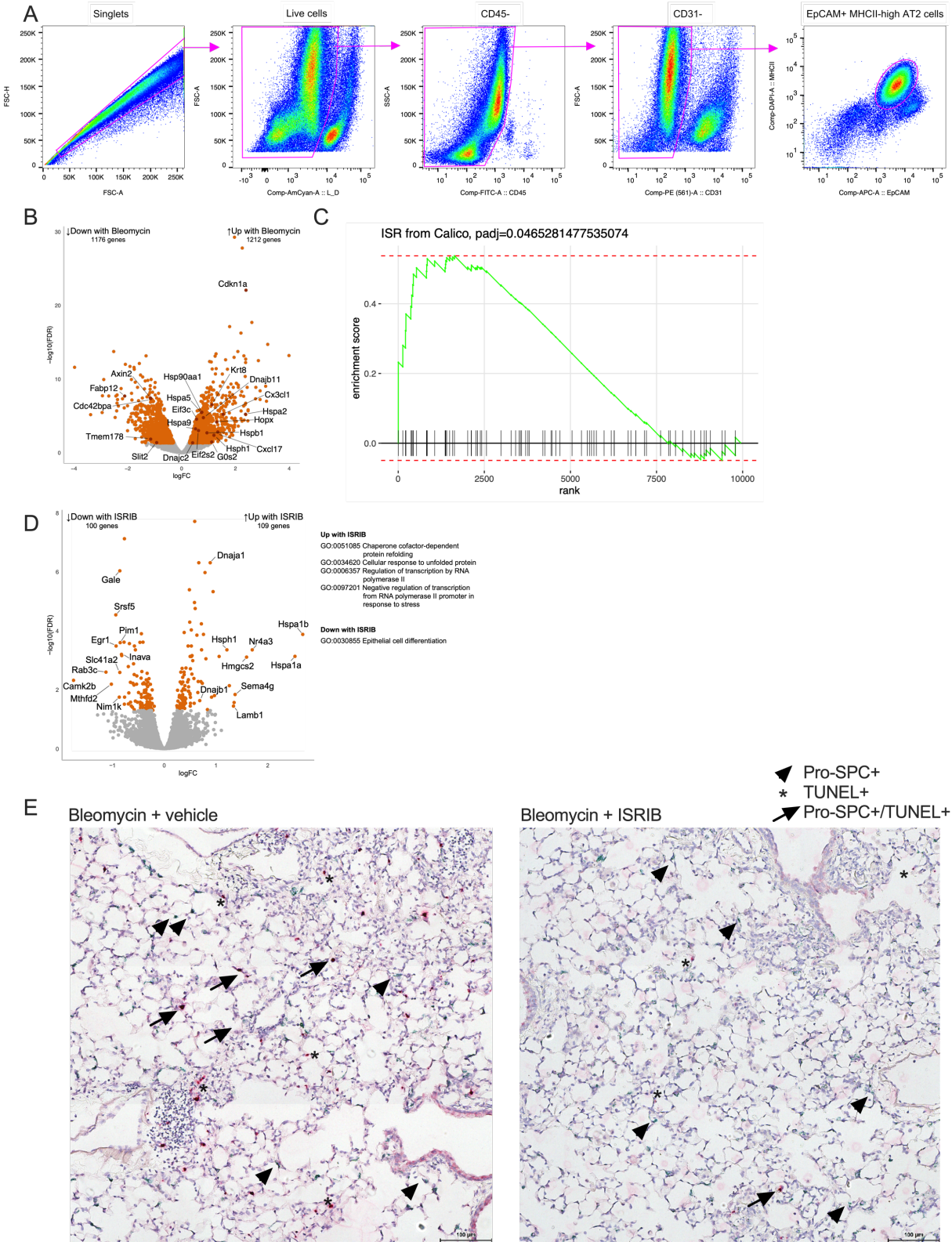


**Figure S7. ISRIB ameliorates fibrosis by modulating stress response in epithelial cells. (A)** Representative gating strategy to isolate AT2 cells by flow sorting. **(B)** Volcano plot showing up- and down-regulated genes in AT2 cells 14 days after treatment with bleomycin (FDR q-value < 0.05). **(C)** GSEA

enrichment plot of genes related to integrated stress response in AT2 cells after treatment with bleomycin (44). **(D)** Volcano plot showing up- and down-regulated genes in AT2 cells in young naïve mice 24 hours after a single dose of ISRIB. **(E)** Representative microphotographs of lung tissue stained for TUNEL and prosurfactant protein C (Pro-SPC). Mice received intratracheal administration of bleomycin at day 0, were treated with vehicle or ISRIB on day 7 and analyzed on day 10. Arrowheads indicate Pro-SPC<sup>+</sup> AT2 cells. Asterisks indicate TUNEL<sup>+</sup> apoptotic cells. Arrows indicate TUNEL<sup>+</sup>Pro-SPC<sup>+</sup> apoptotic AT2 cells. Scale bar = 100µm.

**Supplemental Table S1: Key Resources Table**

REAGENT or RESOURCE	SOURCE	IDENTIFIER
<b>Antibodies</b>		
Rat anti-mouse I-A/I-E (MHC II), BUV395	BD Biosciences	Cat# 743876, RRID:AB_2741827
Rat anti-mouse CD24, BUV496	BD Biosciences	Cat#564664, RRID:AB_2716853
Rat anti-mouse CD11b, BUV737	BD Biosciences	Cat#564443, RRID:AB_2738811
Rat anti-mouse Ly-6C, eFluor 450	eBioscience	Cat#48-5932-82, RRID:AB_10805519
Mouse anti-mouse CD64, PE	BioLegend	Cat#139303, RRID:AB_10613467
Mouse anti-mouse NK-1.1, PE-CF594	BD Biosciences	Cat#562864, RRID:AB_2737850
Hamster anti-mouse CD11c, PE-Cy7	BD Biosciences	Cat#558079, RRID:AB_647251
Rat anti-mouse Siglec F, Alexa Fluor 647	BD Biosciences	Cat#562680, RRID:AB_2687570
Rat anti-mouse CD45, APC-Cy7	BD Biosciences	Cat#557659, RRID:AB_396774
Rat anti-mouse CD45, FITC	BD Biosciences	Cat#561088, RRID:AB_10562038
Rat anti-mouse CD45, eFluor 450	eBioscience	Cat#48-0451-82, RRID:AB_1518806
Rat anti-mouse Ly-6G, Alexa Fluor 700	BD Biosciences	Cat#561236, RRID:AB_10611860
Armenian hamster anti-mouse CD3e, FITC	eBioscience	Cat#11-0031-82, RRID:AB_464882
Rat anti-mouse CD25, PE	eBioscience	Cat#12-0251-82, RRID:AB_465607
Rat anti-mouse CD8a, PE	BioLegend	Cat#100762, RRID:AB_2564027
Rat anti-mouse CD62L, APC-eFluor 780	eBioscience	Cat#47-0621-82, RRID:AB_1603256
Rat anti-mouse CD19, Alexa Fluor 700	eBioscience	Cat#56-0193-82, RRID:AB_837083
Rat anti-mouse CD4, BUV395	BD Biosciences	Cat#563790, RRID:AB_2738426
Rat anti-mouse CD44, BUV737	BD Biosciences	Cat#564392, RRID:AB_2738785
Rat anti-mouse CD31, PE	BioLegend	Cat#102407, RRID:AB_312902
Hamster anti-mouse gp38 (T1a), PE	BioLegend	Cat#127407, RRID:AB_2161929
Hamster anti-mouse gp38 (T1a), PE-Cy7	BioLegend	Cat#127411, RRID:AB_10613294
Rat anti-mouse EpCAM, PE-Cy7	BioLegend	Cat#118216, RRID:AB_1236477
Rat anti-mouse EpCAM, APC	eBioscience	Cat#17-5791-82, RRID:AB_2716944
Rat anti-mouse Cytokeratin 8 (Krt8)	DSHB	Cat# TROMA-I, RRID:AB_531826
Rabbit anti-mouse Pro-SPC	Millipore	Cat#AB3786, RRID:AB_91588
Goat anti-mouse Podoplanin	R&D systems	Cat#AF3244, RRID:AB_2268062
Donkey anti-rabbit Alexa Fluor 488	Thermo Fisher Scientific	Cat#A21206, RRID:AB_2535792
Donkey anti-goat IgG AF568	Thermo Fisher Scientific	Cat#A11057, RRID:AB_2534104
Donkey anti-Rat Alexa Fluor 647	Abcam	Cat#ab150155, RRID:AB_2813835
<b>Chemicals, Peptides, and Recombinant Proteins</b>		
Bleomycin	Fresenius Kabi	Cat#0703-3154-01
Asbestos (UICC crocidolite)	Provided by US Environmental Protection Agency	
ISRIB	AdooQ BioScience	Cat#A14302
<b>Critical Commercial Assays</b>		
EdU	ThermoFisher Scientific	Cat#C10044
Click-iT Plus EdU Alexa Fluor 647 Flow Cytometry Assay Kit	ThermoFisher Scientific	Cat#C10634
PicoPure RNA Isolation Kit	ThermoFisher Scientific	Cat#KIT0204
AllPrep DNA/RNA Mini Kit	Qiagen	Cat#80204
NEBNext RNA Ultra I kit	New England Biolabs	Cat#E7530L
polyA mRNA isolation module	New England Biolabs	Cat#E7490S

SMARTer Stranded Total RNA-Seq Kit v2 - Pico Input Mammalian kit	Takara Bio	Cat#634413
<b>Deposited Data</b>		
Bulk RNA-seq	This study	GSE145295, GSE145590, GSE145771
Experimental Models: Organisms/Strains		
Mouse: C57BL/6J (8-12 weeks old)	The Jackson Laboratory	JAX: 000664
Mouse: C57BL/6J (over 18 months old)	National Institute of Aging	
Mouse: Cx3cr1ERCre	The Jackson Laboratory	JAX: 020940
Mouse: SftpcERCre	The Jackson Laboratory	JAX: 028054
Mouse: ZsGreen	The Jackson Laboratory	JAX: 007906
<b>Software and Algorithms</b>		
ImageJ	Schneider et al., 2012	<a href="https://imagej.nih.gov/ij/">https://imagej.nih.gov/ij/</a>
bcl2fastq 2.19.1		<a href="https://support.illumina.com/sequencing/sequencing_software/bcl2fastq-conversion-software.html">https://support.illumina.com/sequencing/sequencing_software/bcl2fastq-conversion-software.html</a>
FastQC		<a href="https://www.bioinformatics.babraham.ac.uk/projects/fastqc/">https://www.bioinformatics.babraham.ac.uk/projects/fastqc/</a>
Trimmomatic 0.36		<a href="http://www.usadellab.org/cms/?page=trimmomatic">http://www.usadellab.org/cms/?page=trimmomatic</a>
STAR 2.6.0	Dobin et al., 2013	<a href="https://github.com/alexdobin/STAR">https://github.com/alexdobin/STAR</a>
htseq-count 0.11.2	Anders et al., 2014	<a href="https://htseq.readthedocs.io/en/latest/">https://htseq.readthedocs.io/en/latest/</a>
edgeR 3.28.0	Robinson, 2010	

## LIST OF SUPPLEMENTAL DATASETS

**Dataset S1:** Number of differentially-expressed genes between young/old ISRIB/vehicle samples of sorted monocytes. Related to Figure S6A.

**Dataset S2:** List of differentially-expressed genes, their clusters and statistics from Figure 6A.

**Dataset S3:** List of GO biological processes for each cluster in Figure 6A.

**Dataset S4:** List of differentially-expressed genes and their statistics from Figure 7B.

**Dataset S5:** List of differentially-expressed genes and their statistics from Figure 7D.